Growth of gold nanoparticles at gelatin-silica bio-interfaces

Imen Bensaid, Sylvie Masse, Mohamed Selmane, Shemseddine Fessi, Thibaud Coradin

AIP | APL Materials

Growth of gold nanoparticles at gelatin-silica bio-interfaces

Imen Bensaid, Sylvie Masse, Mohamed Selmane, Shemseddine Fessi, and Thibaud Coradin

Citation: APL Mater. **4**, 015704 (2016); doi: 10.1063/1.4935309
View online: http://dx.doi.org/10.1063/1.4935309
View Table of Contents: http://scitation.aip.org/content/aip/journal/aplmater/4/1?ver=pdfcov
Published by the AIP Publishing

Growth of gold nanoparticles at gelatin-silica bio-interfaces

Imen Bensaid,[1,2] Sylvie Masse,[1] Mohamed Selmane,[1] Shemseddine Fessi,[3] and Thibaud Coradin[1,a]

[1]*Sorbonne Universités, UPMC Univ Paris 06, CNRS, Collège de France, Laboratoire de Chimie de la Matière Condensée de Paris, 11 Place Marcelin Berthelot, 75005 Paris, France*
[2]*Unité de Recherche Synthèse et Structure de Nanomatériaux, Faculté des Sciences de Bizerte, 7021 Jarzouna, Tunisia*
[3]*Laboratoire de Chimie des Matériaux et Catalyse, Département de Chimie, Faculté des Sciences de Tunis, Campus Universitaire de Tunis El Manar, 2092 Tunis, Tunisia*

(Received 28 July 2015; accepted 26 October 2015; published online 4 November 2015)

The growth of gold nanoparticles via chemical reduction of $HAuCl_4$ dispersed in gelatin-silicate mixtures was studied. Gelatin leads to densely packed nanoparticles whereas open colloidal aggregates with tight boundaries are formed within silica. Within the bio-hybrid systems, gold species are located within the gelatin-silicate particles and/or within the gelatin phase, depending on the preparation conditions. These various localizations and their impact on the final nanoparticle structure are discussed considering attractive and repulsive electrostatic interactions existing between the three components. These data suggest that bio-hybrid systems are interesting and versatile interfaces to study crystallization processes in confined environments. [http://dx.doi.org/10.1063/1.4935309]

Extracellular matrices (ECMs) play a key role in the control of mineral particle growth by living organisms.[1] On this basis, many biopolymer-based hydrogels have been used as biomimetic media to reproduce the conditions of formation of biogenic inorganic solids, such as calcium carbonate[2] or hydroxyapatite.[3] Later on, this approach was extended to a wide range of metal and metal oxide nanoparticles.[4] These studies evidenced that the mineralization process depends as much on the chemistry of the biomacromolecules that drives their interaction with the inorganic precursor at the nucleation stage, than on the physics of the soft network, that control the size and shape of the growing particles.[5,6] Similar studies have been performed using inorganic hydrogels, mainly silica, obtained by the sol-gel process.[7,8] Although these approaches have no direct relevance for biomineralization processes, they sometimes lead to highly complex structures that have striking resemblances with biogenic materials.[9]

In this study, we aimed at exploring the influence of a biohybrid system combining a biomacromolecular and a silica network on the formation of inorganic nanoparticles. The interactions between silica and biopolymers have been widely studied in a biomimetic perspective and for the formation of biomaterials.[10,11] We selected gelatin as the biological polymer because it interacts strongly with silica via electrostatic interactions, leading to an intimate bio-mineral interface.[12] Using gold nanoparticles as probes to investigate crystallization processes, we demonstrate that the localization of the gold precursors within gelatin-silicate mixtures is controlled by their interactions with the two matrix components as well as by the bio-mineral interactions. They define the environment where the reduction reaction occurs and therefore impact on the final size and structure of the gold colloids.

[a]Author to whom correspondence should be addressed. Electronic mail: thibaud.coradin@upmc.fr

TABLE I. Main experimental conditions and macroscopic aspect of the investigated systems.

Sample	SiO_2 (wt. %)	$HAuCl_4$ in	Final product
AuG	0	Gelatin	Purple gel
AuSi-1	0.2	Silicates	Purple solution
AuSi-2	1.0	Silicates	Dark precipitate
AuGSi-1	0.2	Gelatin	Pink gel
AuGSi-2	1.0	Gelatin	Purple gel
AuSiG-1	0.2	Silicates	Purple gel
AuSiG-2	1.0	Silicates	Purple gel

For materials preparation, gelatin (type B, 4 wt. %) and sodium silicate ($Na_2Si_3O_7$) solutions were prepared in deionized water at 37 °C and acidified to pH 5 using HCl.[12] In a first series of experiments, $HAuCl_4$ was added to the gelatin solution (final [Au] = 5×10^{-4}M), mixed for 30 min and an equal volume of the silicate solution was then added under stirring. After 30 min, further addition of hydrazine (final concentration 1.5×10^{-3}M) as a reducing agent was performed. The mixture was left to react for 30 min and then placed in a cold water bath for 24 h. In a second set of experiments, the same procedure was followed except that $HAuCl_4$ was added to the silicate solution. Reference samples were obtained through the same procedure but adding acidified water instead of silicate or gelatin solutions to the $HAuCl_4$-gelatin or $HAuCl_4$-silicate solutions, respectively. Table I gathers these experimental conditions together with main visual features of the obtained products.

When sufficient material was recovered, the samples were air-dried and powders were studied by wide angle X-ray scattering (WAXS) using a S-MAX3000 equipment from RIGAKU (CuK_α radiation = 1.540 56 Å) with an image plate detector (Fig. 1(a)). For all samples, the diffraction peaks at $2\theta = 38°$ and 44° corresponding to Au cfc (111) and (200) lines, respectively, could be detected. For silicate-rich samples, the diffractions peaks of NaCl resulting from neutralization of $Na_2Si_3O_7$ with HCl were also detected. When samples are compared, it can be noticed that diffractions peaks of the gold phase in AuGSi samples have a larger line width (i.e., have a smaller crystallite size) than within pure gelatin, with AuSiG powders presenting an intermediate situation.

UV-visible spectra of the samples were also recorded on a Uvikon XS spectrophotometer (Fig. 1(b)). AuG, AuGSi-2, and AuSiG-1 show broad plasmon bands whereas much better resolved peaks were obtained for the two other samples. In terms of maximum wavelength of absorption, the highest value was found for pure gelatin (ca. 580 nm) and the lowest for AuGSi-1 (ca. 545 nm). AuSiG-1 had maximum wavelength closer the former (ca. 565 nm) and AuGSi-2 and AuSiG-2 to the latter (ca. 550 nm). It is important to point out that the UV-visible spectra of AuGSi and AuSiG samples in the sol state (i.e., before cooling) were similar to those of the final gel samples (data not shown), indicating that the gelation process had no influence on the optical properties of the gold particles. As a common trend, a narrow plasmon band at high energy indicates well-dispersed

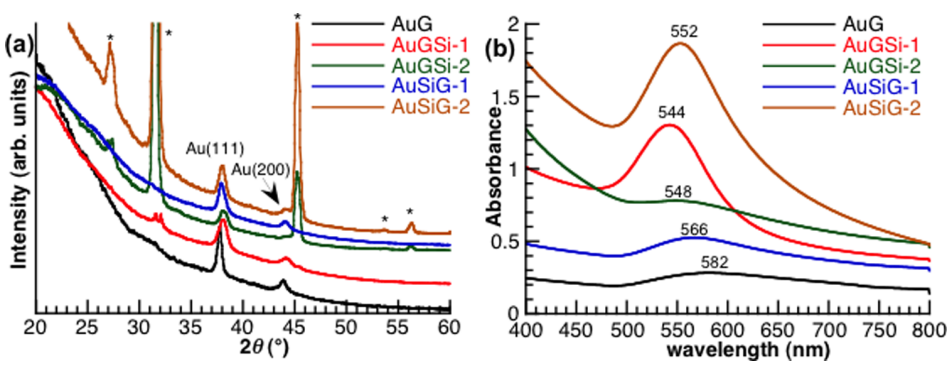

FIG. 1. (a) XRD patterns of the freeze-dried samples and (b) UV-visible absorption spectra of gels.

small particles whereas a broad plasmon band at low energy corresponds to particle aggregates.[13] In the case of aqueous suspensions of dispersed gold nanoparticles, maximum wavelength of 550 nm corresponds to ca. 80 nm colloids and plamson resonance at 580 nm to ca. 100 nm particles.[14] However, it must be pointed out that both silica and gelatin coatings have been shown to induce a blue-shift the maximum of plasmon resonance band of gold nanoparticles compared to aqueous solutions due to change of the dielectric properties of the particle environments.[15,16]

Examination of the AuG sample using transmission electron microscopy (TEM, performed on TECNAI Spirit G2 microscope at a 120 kV working voltage) showed that it mainly consists of spherical dense aggregates (average size 50-100 nm) of nanoparticles 5-10 nm in diameter associated with the gelatin phase (Fig. 2(a) and Fig. S1 of the supplementary material[17]). For AuSi-1 and AuSi-2, particles of 40 ± 10 nm formed open aggregates associated with the silica phase (Figs. 2(b) and S1[17]). At higher magnification, it is possible to observe that a very tight boundary exist between these nanoparticles (Fig. 2(c)). In both cases, EDAX and electron diffraction analysis confirm that these particles correspond to crystalline gold nanoparticles (Figures S2 and S3 of the supplementary material).[17] For AuGSi-1, large particles (50-100 nm) were sometimes observed in the gelatin networks but most gold colloids with size 15 ± 5 nm were observed associated with the dense silica-rich grains; electron diffraction confirms the XRD data suggesting low crystallinity of these particles (Fig. S3[17]). For AuGSi-2 samples, only the smallest gold nanoparticles were identified associated with the dense grains (Fig. 2(d)). Gold particle distribution within AuSiG-1 samples was highly heterogeneous (Fig. S1[17]) with large particles similar to those observed for pure gelatin and smaller colloids (15 ± 5 nm) whose tight boundaries were reminiscent of pure silica systems (Fig. 2(e)). AuSiG-2 also shows a large size distribution of gold nanoparticles but, at high magnification, it was possible to observe nm-scale dark objects intimately associated with the dense silica phases that were attributed to gold clusters (Fig. 2(f)), although the intensity of the EDAX signals were too low for unambiguous attribution.

We have previously shown that gelatin-silicates mixtures at pH 5 lead to the formation of hybrid particles with a fixed composition of SiO_2: gelatin = 1.5 (w/w) for low mineral and protein content.[12] This reaction leads to a depletion of the solution in free gelatin so that the final product is either a gel if the remaining protein concentration is sufficient or a precipitate if it decreases below the minimum gelation concentration. The former situation was observed for all hybrid samples obtained in this work so that gold particle formation can occur in two different environments, pure gelatin or silica-gelatin hybrid networks. However, because $HAuCl_4$ is added before mixing the two solutions and addition of hydrazine, no significant difference between the two studied protocols was expected.

Investigation of the single systems showed two distinct phenomena. Gelatin favors the formation of well-crystallized gold nanocrystals that aggregate into larger densely packed particles. This is in agreement with the literature showing that gelatin can act as a glue to assemble grown gold nanoparticles.[18] In contrast, silicates lead to open aggregates of small colloids exhibiting

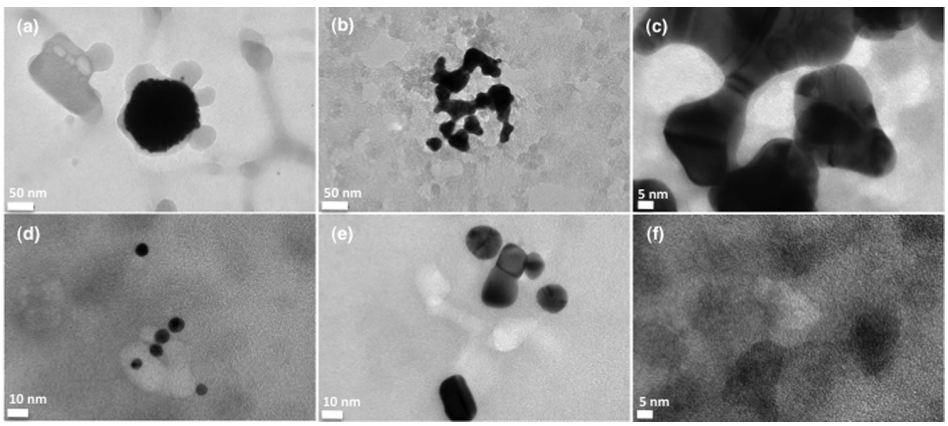

FIG. 2. TEM images of (a) AuG, ((b) and (c)) AuSi-1, (d) AuGSi-2, (e) AuSiG-1, and (f) AuSiG-2 samples.

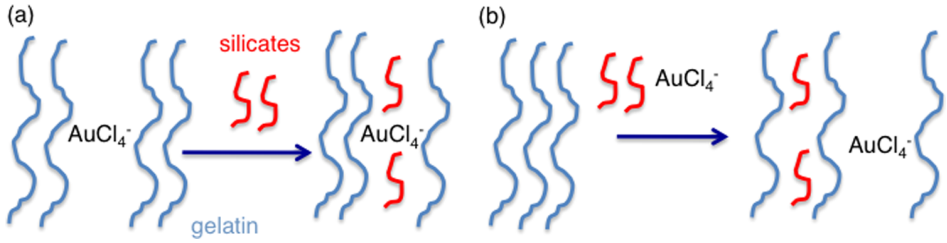

FIG. 3. Schematic illustration of the impact of experimental procedure on the localization of gold species upon silicification: (a) gelatin-stabilized $AuCl_4^-$ remain trapped within the hybrid particles; (b) unstabilized $AuCl_4^-$ are expelled from silicate proximity and migrate to the gelatin phase.

tight boundaries, suggesting unfavorable growth of gold particles within the silica matrix. This difference can be understood considering that upon dissolution, $HAuCl_4$ dissociates into H^+ and $AuCl_4^-$ species. At pH 5, gelatin is positively charged and therefore interacts favorably with gold species via attractive electrostatic interactions.[19] In contrast, poly-silicic acids (i.e., silicate oligomers) are negatively charged at this pH, leading to unfavorable repulsive electrostatic interactions with anionic gold species. For hybrid systems, the co-existence of large and small particles is observed but the balance between these two populations and the size of the silica-associated particles varies with silicate content and order of addition. Intragranular particles obtained for silicate addition to $AuCl_4^-$/gelatin mixtures are very much alike gold colloids forming the dense aggregates found in pure gelatin. This suggests that this reaction corresponds to the silicification of the metal-biopolymer system (Figure 3(a)).[20] For gelatin addition to $AuCl_4^-$/silicates at low concentration, the intragranular particles resemble that of pure silicate systems. However, at higher silicate concentrations, the size of these particles decreases down to a cluster size whereas more particles are found in the gelatin phase. This suggests that gold ions are expelled from their inorganic environment when the gelatin-silicate reaction occurs (Figure 3(b)).

As a conclusion, we have investigated here a ternary hybrid system whose reactivity depends by a subtle balance between attractive and repulsive interactions. The diverging affinity of silicates and gelatin for Au(III) species together with their mutual strong interaction leads to variations in the localization of the gold precursors, as well as in gold particle size and aggregation state depending on the preparation method. This suggests that bio-mineral hybrid systems combining opposite reactivity at the nanometer scale constitute interesting yet unexplored media to study crystallization processes in confined environments.

[1] S. Mann, *Biomineralization* (Oxford University Press, Oxford, 2001).
[2] K. Subburaman, N. Pernodet, S. Y. Kwak, E. DiMasi, S. Ge, V. Zaitsev, X. Ba, N. L. Yang, and N. Rafailovtich, Proc. Natl. Acad. Sci. U. S. A. **103**, 14672 (2006).
[3] F. Nudelman, K. Pieterse, A. George, P. H. Bomans, H. Friedrich, L. J. Brylka, P. A. Hibers, G. de With, and N. A. Sommerdjik, Nat. Mater. **9**, 1004 (2010).
[4] Z. Schnepp, Angew. Chem., Int. Ed. **52**, 1096 (2013).
[5] S. Hall, Proc. R. Soc. A **465**, 335 (2009).
[6] V. Jaouen, R. Brayner, D. Lantiat, N. Steunou, and T. Coradin, Nanotechnology **21**, 185605 (2010).
[7] G. Ennas, A. Musinu, G. Piccaluga, D. Zedda, D. Gatteschi, C. Sangregorio, J. L. Stanger, G. Concas, and G. Spano, Chem. Mater. **10**, 495 (1998).
[8] H.-J. Jeon, S.-C. Yi, and S.-G. Oh, Biomaterials **24**, 492 (2003).
[9] J. M. Garcia-Ruiz, E. Melero-Garcia, and S. T. Hyde, Science **323**, 362 (2009).
[10] S. V. Patwardhan, Chem. Commun. **47**, 7567 (2011).
[11] F. Fernandes, T. Coradin, and C. Aimé, Nanomaterials **4**, 792 (2014).
[12] T. Coradin, S. Bah, and J. Livage, Colloids Surf., B **35**, 53 (2004).
[13] S. K. Ghosh and T. Pal, Chem. Rev. **107**, 4797 (2007).
[14] W. Haiss, N. T. K. Thanh, J. Aveyard, and D. G. Fernig, Anal. Chem. **79**, 4215 (2007).
[15] J. Rodriguez-Fernandez, I. Pastoriza-Santos, J. Perez-Juste, F. J. Garcia de Abajo, and L. M. Liz-Marzan, J. Phys. Chem. C **111**, 13361 (2007).
[16] S. Suarasan, M. Focsan, D. Maniu, and S. Astilean, Colloids Surf., B **103**, 475 (2013).
[17] See supplementary material at http://dx.doi.org/10.1063/1.4935309 for additional TEM images, EDAX analyses, and electron diffraction pattern.
[18] S. Liu, Z. Zhang, and M.-Y. Han, Adv. Mater. **17**, 1862 (2005).
[19] R. Brayner, T. Coradin, M.-J. Vaulay, C. Mangeney, J. Livage, and F. Fiévet, Colloids Surf., A **256**, 191 (2005).
[20] J. Allouche, S. Soulé, J.-C. Dupin, S. Masse, T. Coradin, and H. Martinez, RSC Adv. **4**, 63234 (2014).